Interferometric calibration of deformable mirrors

Jacopo Antonello[*1], Débora Andrade[†1], Brian R. Patton[‡1,2], and Martin J. Booth[§1,2]

[1]Centre for Neural Circuits and Behaviour, University of Oxford, Mansfield Road, Oxford OX1 3SR, UK
[2]Department of Engineering Science, University of Oxford, Parks Road, Oxford OX1 3PJ, UK

Mon Jul 4 17:22:34 2016 +0100
v0.9-19-g8250984-200

1 Theory

1.1 Introduction

(JA: TODO) . . . other methods [1, 2] . . .

1.2 Linear static control of a deformable mirror

We assume that a deformable mirror (DM) with N_a actuators is a linear device. The phase aberration $\Phi(\rho, \theta)$ after reflection from the DM is given by the superposition of the influence functions [3, 4] $\psi_i(\rho, \theta)$ of each actuator, where ρ, θ are the spatial coordinates in the unit disk (pupil), and u_i is the control signal of the i-th actuator

$$\Phi(\rho, \theta) = \sum_{i=1}^{N_a} u_i \psi_i(\rho, \theta). \tag{1}$$

For a suitable number N_z of Zernike polynomials [5] $\mathcal{Z}_j(\rho, \theta)$, the phase aberration is approximated by

$$\Phi(\rho, \theta) \approx \sum_{j=1}^{N_z} z_j \mathcal{Z}_j(\rho, \theta), \tag{2}$$

where z_j is the j-th [6, 7] Zernike coefficient.

The coefficients u_i and z_j are collected respectively into vectors $\mathbf{u} \in \mathbb{R}^{N_a}$ and $\mathbf{z} \in \mathbb{R}^{N_z}$. By considering a grid defined in the pupil, N_c samples of $\Phi(\rho, \theta)$ are collected into a vector $\boldsymbol{\phi} \in \mathbb{R}^{N_c}$.

[*]jacopo.antonello@dpag.ox.ac.uk
[†]debora.andrade@dpag.ox.ac.uk
[‡]brian.patton@cncb.ox.ac.uk
[§]martin.booth@eng.ox.ac.uk

Similarly, we evaluate $\psi_i(\rho,\theta)$ and $\mathcal{Z}_j(\rho,\theta)$ over the grid and define two matrices $\Psi \in \mathbb{R}^{N_c \times N_a}$ and $Z \in \mathbb{R}^{N_c \times N_z}$. Using Eqs. (1) and (2), we find $\boldsymbol{\phi} = \Psi \mathbf{u}$ and $\boldsymbol{\phi} \approx Z\mathbf{z}$.

We would like to recover a matrix H that maps an actuation vector $\mathbf{u}$ into the corresponding vector of Zernike coefficients $\mathbf{z}$, i.e., $\mathbf{z} \approx H\mathbf{u}$. H can be computed using input–output measurements.

1.3 Interferometric measurement of the phase

We use an interferometer like the one depicted in Fig. 6, where the reference mirror is tilted by an angle α. The phase can be covered by applying Fourier-based fringe analysis [8, 9, 10]. The interferogram recorded with the CCD is given by

$$I = |Ae^{i\Phi} + Be^{i\varphi}|^2 = A^2 + B^2 + ABe^{i(\Phi-(\delta_p+c_2x+c_3y))} + ABe^{-i(\Phi-(\delta_p+c_2x+c_3y))}, \qquad (3)$$

where δ_p is the piston difference between the two arms of the interferometer, and $\varphi = c_2x + c_3y$ relates to the tip-tilt α of the reference mirror.

By applying the Fourier transform to Eq. (3), and by considering the spatial-frequencies shifting theorem ($\mathcal{F}[f(\mathbf{x})e^{i2\pi\mathbf{a}^T\mathbf{x}}] = \hat{f}(\mathbf{y}-\mathbf{a})$), we can separate $\mathcal{F}[ABe^{i(\Phi-(\delta_p+c_2x+c_3y))}]$ from the other terms in Eq. (3). The phase $\Phi - \delta_p \mod 2k\pi$ is obtained by applying the following steps:

1. multiply by a mask function
2. shift the origin in the Fourier space
3. inverse Fourier transform
4. apply atan2(·)

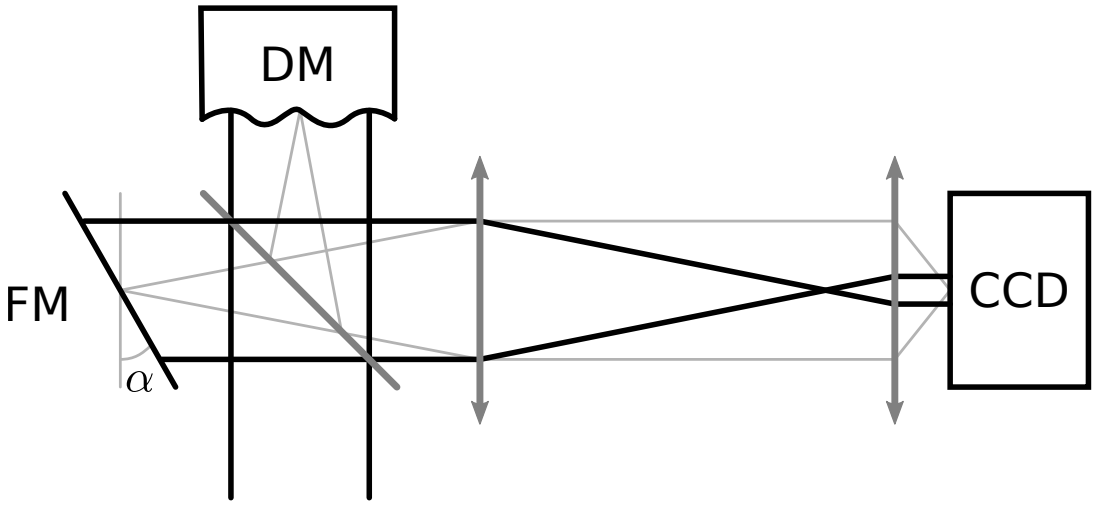

Figure 1: Interferometer setup to calibrate the DM. The reference flat mirror (FM) is tilted by an angle α. A fringe pattern is recorded with the camera (CCD). The camera is conjugated to the DM.

Using this method, one can collect a set of D input-output measurements, i.e., $\boldsymbol{\phi}_1, \ldots, \boldsymbol{\phi}_D$ corresponding to different settings of the deformable mirror $\mathbf{u}_1, \ldots, \mathbf{u}_D$.

(JA: finish fringe analysis section)
(JA: phase unwrapping section)
(JA: piston adjustment section)

1.4 Computation of the influence matrix

Following [11], we compute H by solving the normal equation

$$Z^T Z H (\sum_{i=1}^{D} \mathbf{u}_i \mathbf{u}_i^T) = Z^T (\sum_{i=1}^{D} \boldsymbol{\phi}_i \mathbf{u}_i^T), \tag{4}$$

which involves multiplying from the left and from the right by the inverse matrices of $Z^T Z$ and $\sum_{i=1}^{D} \mathbf{u}_i \mathbf{u}_i^T$. For a properly defined grid, the inverse of $Z^T Z$ exists [12] and $Z^T Z \approx I$, due to the orthogonality property of the Zernike polynomials. Additionally, vectors $\mathbf{u}_i$ can be selected so that $\sum_{i=1}^{D} \mathbf{u}_i \mathbf{u}_i^T$ is full rank. In particular, one can select vectors $\mathbf{u}_i$ from the columns of $[-l, \ldots, l] \otimes I_{N_a}$, to ensure that the condition number of $\sum_{i=1}^{D} \mathbf{u}_i \mathbf{u}_i^T$ is minimal. This corresponds scanning each actuator at a time from $-l$ to l. For example, one can record three measurements for the first actuator, by setting it to -0.6, 0.0 and 0.6, while keeping all other actuators at fixed at the zero position. This operation is then repeated for all remaining actuators until a full dataset is obtained.

- (TODO) piston control section
- (TODO) control matrix section
- (TODO) state feedback section
- (TODO) regularisation section

2 Software

This software can be used to obtain an influence matrix H and the initial aberration z_0 from a set of interferometric measurements. From these, one can also compute the control vector $\mathbf{u}_f$ to flatten the DM, and a control matrix C.

2.1 Requirements

- MATLAB
- Anaconda for Python 3 in Windows or standard Python 3 in Linux
- (OPTIONAL) CVX to be installed into `ext/cvx`

2.2 Dataset format

A dataset of interferometric measurements consists of a directory containing two files for each measurement.

The first file is an ASCII file that contains the vector $\mathbf{u}_i$, and is parsed according to `mlib/labview_read_matrix.m`. It is assumed that each element of $\mathbf{u}_i$ is normalised to $[-1, 1]$, where ± 1

denotes saturation. If a MEMS DM [13, 14] is used, one should use the square root of the voltage as a control variable [4, 15, 16], so that a linear displacement of the mirror is expected. For example, if the voltage v of each actuator varies between 0 and $V_{\max}$, one can use the equation

$$v = V_{\max}\sqrt{(u+1)/2} \tag{5}$$

to relate each element of the control vector $\mathbf{u}_i$ to the corresponding voltage that is effectively applied to the actuator.

The second file contains the corresponding interferogram image, which is parsed according to `mlib/labview_read_dbl.m`. One may use different file formats and conventions by modifying these two functions.

2.3 Selecting the aperture

A dataset can be parsed using `parse_labview_data.m`. This script implements a Fourier-based fringe analysis [8, 10] method, and applies a phase unwrapping algorithm [17] to each measurement. First, one has to select the mask defining the aperture location and size, see Fig. 2 and Fig. 3. Second, the Fourier mask can be selected (Fig. 4), and the result of the Fourier analysis can be examined for the first interferogram measurement (Fig. 5). By default actuators that lie outside of the selected aperture and have little influence on the phase are neglected.

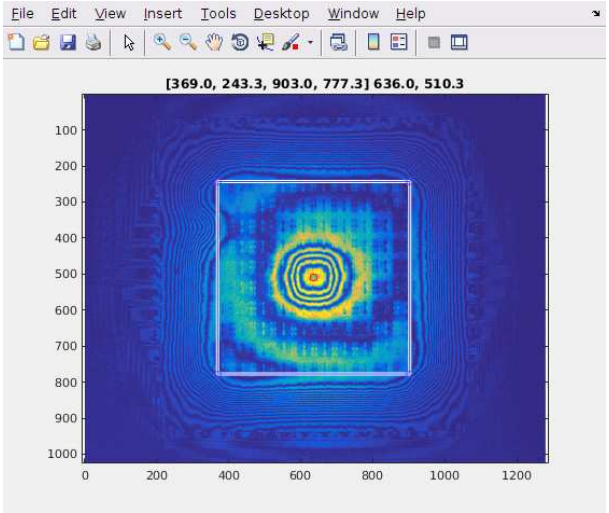

Figure 2: Before tilting the reference mirror, one can record a measurement with no tilt where the central actuator is poked. This measurement is then used to define and align the aperture mask.

2.4 Calibrating the deformable mirror

Once the dataset has been parsed, the calibration is done with `dm_calib.m`. One can choose the maximum radial order for the Zernike polynomials [5], which are normalised and ordered according to [6, 7]. The calibration is performed by solving a least-squares problem, as described in [11]. Note that the ordering, number, and location of the actuators is not important for the calibration, as such information is not necessary to solve Eq. (4). This information is of course

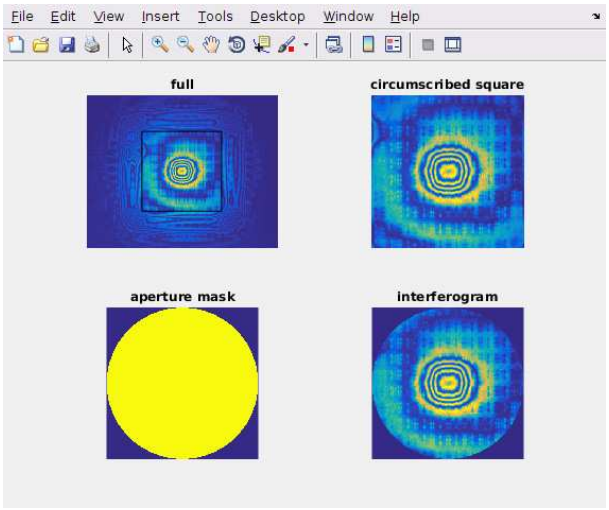

Figure 3: The aperture mask is defined by a bounding box.

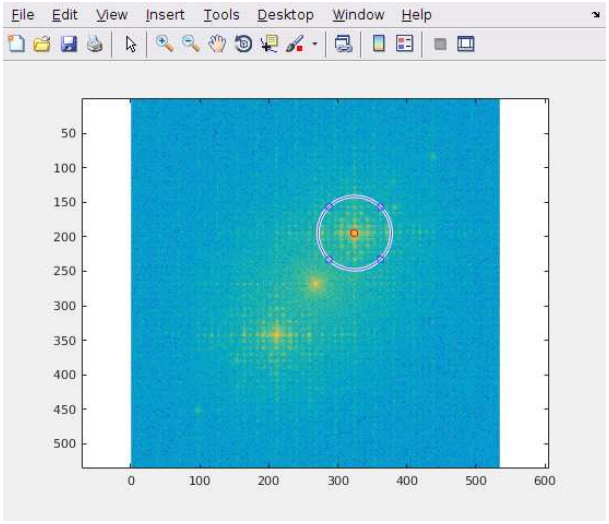

Figure 4: A Fourier mask should be selected around either of the first orders.

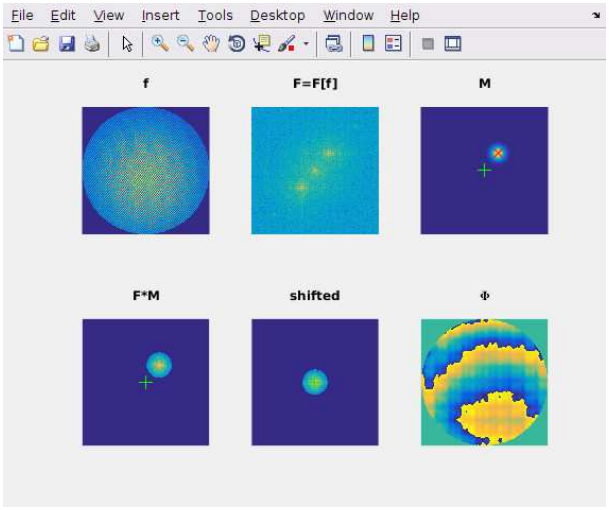

Figure 5: The results of selecting the Fourier mask can be checked on the first interferogram of the dataset.

implicitly present in a dataset. In particular, the graphs depicting the actuator layouts are only a visual aid for debugging purposes, and only provide a gross indication of the membrane shape. If the locations of the actuators is not known, for example when using another kind of deformable mirror other than the Boston Multi-DM 140 or the Mirao 52e (see `modelling/*.m`), then the function `dm_plot.m` cannot be used and the graphs of the actuator layouts are not available. Nevertheless, the calibration can still be completed without such graphs. Note that same ordering convention must be used when acquiring the dataset and afterwards when controlling the mirror.

Once the calibration is completed, it can be checked by trying to make different Zernike shapes with the mirror and by measuring the phase with an interferometer or by examining the corresponding point-spread function. The code in `fringe_analysis.m` can be used to parse the validation data and check how well the Zernike shapes can be reproduced.

In the relationship $\mathbf{z} \approx H\mathbf{u}$, $\mathbf{z}$ is the vector of Zernike coefficients expressed in radians. Therefore the phase

$$\Phi(\rho, \theta) = \sum z_i \mathcal{Z}_i(\rho, \theta). \tag{6}$$

is measured in radians. In particular, if one sets the piston coefficient z_0 to zero, the rms [7] of $\Phi(\rho, \theta)$ is given by the norm of $\mathbf{z}$.

The phase can be related to the wavefront aberration introduced by reflecting off the membrane $W(\rho, \theta)$, expressed for example in µm, using $W = \lambda/(2\pi)\Phi(\rho, \theta)$, where λ is the wavelength used during the calibration of the DM. This corresponds to the effective displacement of the membrane up to a factor of two.

2.5 Computation of mirror modes

`dm_calib.m` ... (JA: TODO) ...

2.6 Example 1

The calibration data is in DBL format and the actuators of the DM are scanned symmetrically around zero, i.e., $[-0.5, 0.0, 0.5]$. The piston mode is ignored.

- `edit parse_labview_data.m`
- uncomment the settings for Example 1

```
% EXAMPLE 1 (bmcmultidm140, without piston)
data_ext = 'dbl';
load_data_func = @labview_read_dbl;
calibdir = '../testdata';
reference_intef = '../testdata/reference-no-tilt.dbl';
calibration_lambda = 532e-9;
```

- copy the last masks file, so that some example masks are automatically selected `copyfile ('../testdata/last_masks.mat', './last_masks.mat')`
- run this script
- `edit dm_calib.m`
- uncomment the settings for Example 1

```
% EXAMPLE 1 (bmcmultidm140, without piston)
datasetpath = 'testdata.mat';
exclude_piston = 1; % fully ignore piston mode for all phase measurements
```

- run this script

2.7 Example 2

The calibration data is in TIFF format and the actuators of the DM are scanned symmetrically around zero, i.e., $[-0.5, 0.0, 0.5]$. The piston mode is ignored.

- `edit parse_labview_data.m`
- uncomment the settings for Example 2

```
% EXAMPLE 2 (bmcmultidm140, with piston)
% actuators symmetrically scanned around 0, e.g., [-.5, -.25, 0, .25, .5]
data_ext = 'tif';
load_data_func = @labview_read_tif;
calibdir = '../testdata-2016-07-04';
reference_intef = '../testdata-2016-07-04/reference-no-tilt.tif';
calibration_lambda = 650e-9;
```

- copy the last masks file, so that some example masks are automatically selected

```
copyfile('../testdata-2016-07-04/last_masks.mat', './last_masks.mat')
```

- run this script
- `edit dm_calib.m`

- uncomment the settings for Example 2

```
% EXAMPLE 2 (bmcmultidm140, with piston)
datasetpath = 'testdata-2016-07-04.mat';
exclude_piston = 0;
```

- run this script

3 Troubleshooting

3.1 Waffle mode

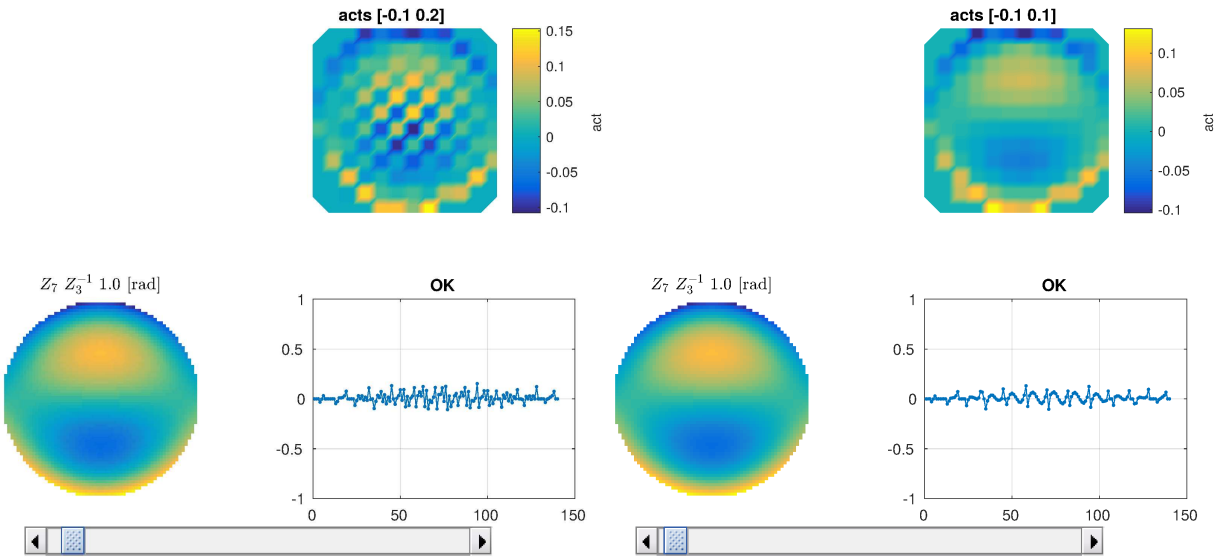

Figure 6: Left: too few Zernike polynomials are used, and the Zernike decomposition approximates the waffle mode error to zero. This error appears though in the control matrix. Right: by using more Zernike polynomials, the waffle mode error is picked up by the decomposition and the waffle mode is not present in the control matrix. (JA: TODO)

References

[1] D. Débarre, T. Vieille, and E. Beaurepaire, "Simple characterisation of a deformable mirror inside a high numerical aperture microscope using phase diversity," J. Microsc. **244**, 136–143 (2011).

[2] M. Booth, T. Wilson, H.-B. Sun, T. Ota, and S. Kawata, "Methods for the characterization of deformable membrane mirrors," Appl. Opt. **44**, 5131–5139 (2005).

[3] C. Paterson, I. Munro, and J. Dainty, "A low cost adaptive optics system using a membrane mirror," Opt. Express **6**, 175–185 (2000).

[4] G. Vdovin, O. Soloviev, M. Loktev, and V. Patlan, *OKO Guide to Adaptive Optics* (Flexible Optical B.V., 2013), 4th ed.

[5] F. Zernike, "Beugungstheorie des Schneidenverfahrens und seiner verbesserten Form, der Phasenkontrastmethode," Physica **1**, 689–704 (1934).

[6] R. J. Noll, "Zernike polynomials and atmospheric turbulence," J. Opt. Soc. Am. **66**, 207–211 (1976).

[7] V. N. Mahajan, "Zernike circle polynomials and optical aberrations of systems with circular pupils," Appl. Opt. **33**, 8121–8124 (1994).

[8] M. Takeda, H. Ina, and S. Kobayashi, "Fourier-transform method of fringe-pattern analysis for computer-based topography and interferometry," J. Opt. Soc. Am. **72**, 156–160 (1982).

[9] M. Peck, "Interferometry mathematics, algorithms, and data," URL. Accessed: 03 Feb 2016.

[10] T. I. M. van Werkhoven, J. Antonello, H. H. Truong, M. Verhaegen, H. C. Gerritsen, and C. U. Keller, "Snapshot coherence-gated direct wavefront sensing for multi-photon microscopy," Opt. Express **22**, 9715–9733 (2014).

[11] J. Antonello, T. van Werkhoven, M. Verhaegen, H. H. Truong, C. U. Keller, and H. C. Gerritsen, "Optimization-based wavefront sensorless adaptive optics for multiphoton microscopy," J. Opt. Soc. Am. A **31**, 1337–1347 (2014).

[12] J. Y. Wang and D. E. Silva, "Wave-front interpretation with zernike polynomials," Appl. Opt. **19**, 1510–1518 (1980).

[13] G. Vdovin and L. Sarro, "Flexible reflecting membranes micromachined in silicon," Semiconductor Science and Technology **9**, 1570 (1994).

[14] T. G. Bifano, R. Krishnamoorthy Mali, J. K. Dorton, J. Perreault, N. Vandelli, M. N. Horenstein, and D. A. Castañon, "Continuous-membrane surface-micromachined silicon deformable mirror," Optical Engineering **36**, 1354–1360 (1997).

[15] J. A. Kubby, ed., *Adaptive Optics for Biological Imaging* (CRC press, 2013).

[16] D. Débarre, M. J. Booth, and T. Wilson, "Image based adaptive optics through optimisation of low spatial frequencies," Opt. Express **15**, 8176–8190 (2007).

[17] M. A. Herráez, D. R. Burton, M. J. Lalor, and M. A. Gdeisat, "Fast two-dimensional phase-unwrapping algorithm based on sorting by reliability following a noncontinuous path," Appl. Opt. **41**, 7437–7444 (2002).